Optimal phase estimation in the presence of correlated dephasing

Srijon Ghosh*[1,2,3], Arkadiusz Kobus*[1,4], Stanisław Kurdziałek[1], and Rafał Demkowicz-Dobrzański[1]

[1]Faculty of Physics, University of Warsaw, Pasteura 5, 02-093 Warszawa, Poland
[2]Dipartimento di Ingegneria, Università di Palermo, Viale delle Scienze, 90128 Palermo, Italy
[3]Institute of Fundamental and Frontier Sciences, University of Electronic Sciences and Technology of China, Chengdu 611731, China
[4]Institute of Physics PAS, Aleja Lotników 32/46, 02-668 Warszawa, Poland

arXiv:2511.07211v3 [quant-ph] 23 Oct 2026

We investigate optimal metrological protocols for phase estimation in the presence of correlated dephasing noise, including spin-squeezed state sensing strategies as well as parallel and adaptive protocols optimized using tensor-network-based numerical methods. The results are benchmarked against fundamental bounds obtained either via the latest quantum comb extension method or an optimized classical simulation method. We find that the spin-squeezed states offer practically optimal performance in the regime where phase fluctuations are positively correlated but can be outperformed by tensor-network-optimized strategies for negatively correlated fluctuations.

1 Introduction

A fundamental challenge in theoretical quantum metrology [1,2,3,4,5,6,7,8,9,10,11] lies in identifying the optimal estimation scheme that achieves the highest precision, when the sensing probes experience realistic noise. Addressing this challenge is of profound importance, both from a fundamental as well as a practical perspective, as it impacts the advancement of practical quantum sensing technologies [6,12,13,14,15,16].

While in ideal noiseless scenarios, proper use of quantum mechanical resources, such as coherence or entanglement, may lead to the famous Heisenberg scaling of precision [1, 2, 17, 18, 19], in the presence of noise, those quantum-enhanced gains, while still possible, are less spectacular, and require more careful design of the metrological protocols [19,20,21,22,23,24,25]

Mathematically, the problem of identifying an optimal sensing strategy may be framed as a quantum channel estimation problem, where the parameter θ is encoded in a quantum channel Λ_θ. The problem is at the same time most challenging and interesting from a practical perspective, when the task involves the use of multiple quantum channels, which may be uncorrelated, correlated spatially, temporally, or both [26,27,28,29,30,31,32,33,34,35,36,37,38,39,40,41,42,43]. For uncorrelated channel estimation models, the problem may be formally regarded as solved, as both asymptotically tight fundamental bounds are known as well as the optimal schemes saturating them [19,20,21,22,23,24,25,44,45,46,47].

In a more general scenario, the noise channels are likely to exhibit correlations. However, characterizing and analyzing correlated quantum channels is a non-trivial task, and the aforementioned bounds and strategies do not, in general, prove useful in this setting. However, more recently, a lot of progress has been made in developing methods to deal with correlated metrological noise models as well [34,48,49,50,51,52,53]. Still, universal constructions of optimal protocols are not known, while the efficiently computable bounds are not guaranteed to be tight in general. To the best of our knowledge, the most recent works [51,52] have focused on the toy model of binary correlated dephasing. Precisely, the two adjacent quantum channels are correlated via only two possible values of the rotation angles.

In this work, we move beyond the binary picture, allowing the correlations between quantum channels to vary continuously. Precisely, we fo-

*These authors contributed equally to this work

cus on a paradigmatic metrological model with correlated noise—phase estimation in the presence of correlated dephasing—where the character of noise may be varied continuously, changing it from anti-correlated noise, via uncorrelated (independent dephasing), up to the fully correlated one (collective dephasing). In this scenario, to derive the fundamental upper bounds of the Fisher information, we use *classical simulation* (CS) [21, 45] method. At first, we calculate a tighter upper bound of the Fisher information by using CS method for the *continuous correlated model* as well as by using the quantum comb extension method [52]. We apply the latest tensor-network-based numerical methods [50, 51] to find the optimal parallel as well as adaptive protocols with up to $N \approx 30$ channels, and compare their performance with basic spin-squeezed state-based strategies, for different character of noise correlations by invoking the Rouwenhorst method of discretizing a continuous noise-model.

The paper is organized as follows. In Sec. 2, we formulate the model of phase estimation in the presence of correlated phase fluctuations. In Sec. 3 we analyze the performance of a parallel channel estimation strategy involving spin-squeezed states and simple measurements in the presence of correlated dephasing. In order to obtain a benchmark for optimality, we derive general bounds on precision with correlated noise using classical simulation method in Sec. 4. In Sec. 5, we present numerical results on protocols optimized with the help of tensor network methods, which are supplemented by numerically obtained fundamental bounds obtained using the quantum comb extension method. Finally, conclusions are drawn in Sec. 6.

2 Phase estimation under the correlated dephasing problem

Let us start with a simple physical motivation for the model, which will be the main focus of this paper. Imagine sensing of a time-varying magnetic field $B(t)$ that is fluctuating around some stable mean value B_0. Consider an elementary two-level quantum system that couples to the magnetic field via a standard Hamiltonian:

$$H_\omega(t) = \frac{1}{2}\mu B(t)\sigma_z = \frac{1}{2}\omega(t)\sigma_z, \tag{1}$$

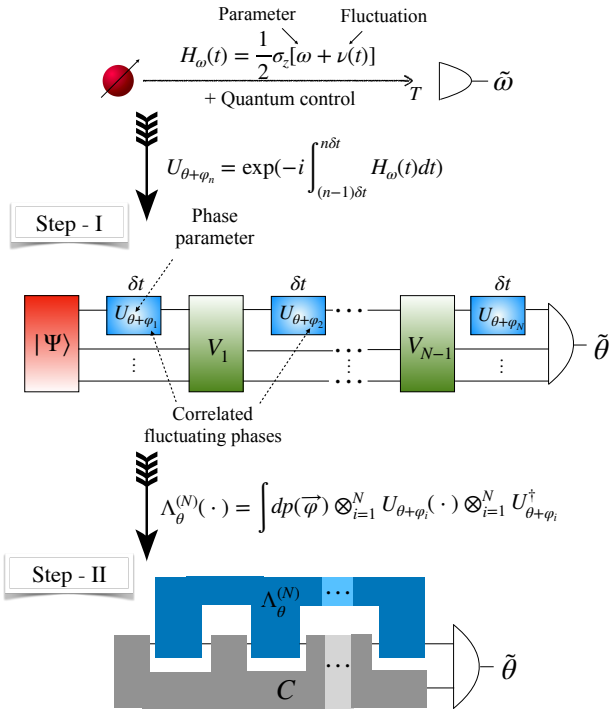

Figure 1: Schematic diagram of a metrological channel estimation protocol with continuous temporal correlations. The continuous-time frequency estimation problem is illustrated at the top, where T denotes the total evolution time. **Step I** represents the mapping of this problem onto a general *discrete-time phase sensing protocol* comprising N steps (middle), where each step involves sensing for a duration δt, followed by a quantum control operation V_n, with $n = 1, 2, \ldots, N-1$. **Step II** involves averaging over noise processes and represents mathematically both the resulting sensing dynamics $\Lambda_\theta^{(N)}$ and the overall control protocol C as quantum combs (bottom).

where μ is the coupling constant (magnetic moment), while $\omega(t)$ is the corresponding Larmor frequency. We may therefore view the problem as effectively a frequency estimation problem,

$$\omega(t) = \omega + \nu(t), \tag{2}$$

where the goal is to estimate ω in the presence of frequency fluctuations denoted here by $\nu(t)$. We allow the system to be subject to arbitrary controls during sensing and, in principle, also entangled with ancillary systems; see Fig. 1.

In order to effectively analyze the model, we assume sensing steps last δt and are intertwined with control operations V_n. We may then view the problem as a phase estimation problem, with

sequential application of unitary operations,

$$U_{\theta+\varphi_n} = \mathrm{e}^{-\mathrm{i}\frac{1}{2}(\theta+\varphi_n)\sigma_z},\ \theta = \omega\delta t,\ \varphi_n = \int_{t_n}^{t_{n+1}} \nu(t)\mathrm{d}t, \tag{3}$$

where φ_n represents the total phase fluctuations accumulated from time $t_n = (n-1)\delta t$ to $t_{n+1} = n\delta t$. The goal is to optimally estimate phase θ, which directly translates to estimation of ω. What makes the problem non-trivial is that we allow for arbitrary controls that may be applied between the applications of the unitaries. If the fluctuating phases φ_n are independent, we would end up with the standard uncorrelated dephasing model, for which it is known that a squeezed-state-based sensing protocol performs optimally [20,21,54,55]. The problem becomes highly non-trivial, however, if fluctuating phases φ_n manifest correlations. Better understanding of this case is the main purpose of this paper.

We will consider the simplest model that is sufficient to study the effect of dephasing correlations, where the vector of subsequent phases $\vec{\varphi} = [\varphi_1, \varphi_2, ...]^T$ is normally distributed,

$$\vec{\varphi} \sim \mathcal{N}(0, \Sigma), \quad \Sigma_{ij} = \sigma^2 c^{|i-j|}, \tag{4}$$

with Σ being the covariance matrix, $c \in (-1, 1)$ being the noise correlation parameter and σ being the noise strength. This assumption makes the model Markovian, and the conditional probability of observing phase φ_{n+1} given φ_n in the previous step reads:

$$\varphi_{n+1}|\varphi_n \sim c\varphi_n + \mathcal{N}\left(0, \sigma^2(1-c^2)\right), \tag{5}$$

A similar type of model would arise when integrating a natural frequency estimation model, where the frequency fluctuations are governed by the Ornstein-Uhlenbeck process [56,57,58,59,60], see Appendix A—in this case though, one would be restricted to positive correlations only, $c \geq 0$, while here we allow for negative correlations as well—such correlation may appear in underdamped models with overshoot-type relaxations or in other oscillating models [61,62].

We may now state the problem formally, as a channel estimation problem, where the θ parameter to be estimated is encoded in the effective channel:

$$\Lambda_\theta^{(N)}(\cdot) = \int \mathrm{d}p(\vec{\varphi}) \left(\bigotimes_{n=1}^{N} U_{\theta+\varphi_n}\right)(\cdot)\left(\bigotimes_{n=1}^{N} U_{\theta+\varphi_n}\right)^\dagger, \tag{6}$$

where $p(\vec{\varphi})$ is the N-variate Gaussian distribution (4). This channel may be viewed as acting on an N-qubit input probe state $\rho^{(N)}$, in which case it will represent a parallel sensing strategy, where the output state is $\rho_\theta^{(N)} = \Lambda_\theta^{(N)}(\rho^{(N)})$. More generally, it may be viewed as a quantum comb [63], with N-qubit inputs and N-qubit outputs, that may be used in a general adaptive strategy as depicted in Fig. 1. In the latter case, the probe-control strategy will be mathematically described by a complementary quantum comb C, while the output state of the protocol will be obtained via a concatenation of the two combs (the link product) $\rho_\theta^{(N)} = \Lambda_\theta^{(N)} \star C$ [51,63].

In this work, we will quantify the performance of the protocol via the *quantum Fisher information (QFI)* [64,65] of the protocol output state $\mathcal{F}_Q(\rho_\theta^{(N)})$. The QFI is defined as:

$$\mathcal{F}_Q(\rho_\theta) = \mathrm{Tr}(\rho_\theta L_\theta^2), \quad 2\dot{\rho}_\theta = L_\theta\rho_\theta + \rho_\theta L_\theta, \tag{7}$$

where L_θ denotes the symmetric logarithmic derivative (SLD) and $\dot{X} = \partial_\theta X$. QFI provides the ultimate lower bound on the estimation variance of θ through the quantum Cramér-Rao (CR) inequality:

$$\mathrm{Var}(\hat{\theta}) \geq \frac{1}{\mathcal{F}_Q(\rho_\theta)}, \tag{8}$$

valid for any measurements and locally unbiased estimators.

In the case of parallel protocols, the optimal protocol will correspond to the choice of the N-probe input state (potentially also entangled with ancillary systems) for which the output QFI is maximized

$$\mathcal{F}_{Q,\mathrm{parallel}}^{(N)} = \max_{\rho^{(N)}} \mathcal{F}_Q[\Lambda_\theta^{(N)}(\rho^{(N)})]. \tag{9}$$

More generally, in the case of adaptive strategies, the maximization should be performed over all legitimate quantum combs C:

$$\mathcal{F}_{Q,\mathrm{adaptive}}^{(N)} = \max_{C} \mathcal{F}_Q[\Lambda_\theta^{(N)} \star C]. \tag{10}$$

If ancillary systems involved in the adaptive strategy are not restricted, the parallel strategy may always be regarded as a special case of the adaptive strategy, and so $\mathcal{F}_{Q,\mathrm{adaptive}}^{(N)} \geq \mathcal{F}_{Q,\mathrm{parallel}}^{(N)}$.

Performing exact optimizations in (9,10), quickly becomes infeasible with growing N, due to the exponential growth of the total Hilbert space dimension involved. In this case, one

needs to consider either some particular educated guessed protocols, or perform numerical optimization using efficient descriptions involving tensor-network methods, modeling entangled states as matrix product states (MPS) in parallel protocols [66], or decomposing general quantum combs into elementary steps, connected via ancillary systems of small dimensions [50, 51]. In the end, these results need to be accompanied by upper bounds, that allow to assess how big the potential gap is between the protocols found and the best possible ones. In the next section, we analyze the performance of the basic parallel phase estimation strategy, where quantum precision enhancement is achieved thanks to spin-squeezing, which is known to be optimal in for the problem of phase estimation in the presence of uncorrelated dephasing [20, 21, 54, 67, 68, 69].

3 Phase estimation using squeezed states

Consider the N- qubit input state in the parallel protocol to be the one-axis twisting *spin-squeezed (SS) state* [68], $\rho^{(N)} = |\mathrm{SS}\rangle\langle\mathrm{SS}|$:

$$|\mathrm{SS}\rangle = e^{\mathrm{i}\varepsilon J_x} e^{-\mathrm{i}\chi J_z^2} |+\rangle^{\otimes N}, \quad J_\alpha = \frac{1}{2}\sum_{n=1}^{N} \sigma_\alpha^{(n)}, \tag{11}$$

where $\sigma_\alpha^{(n)}$ represents a Pauli matrix acting on the n-th qubit, and the squeezing strength $\chi = N^{-3/4}$ as well as the additional state rotation $\varepsilon = \pi/2 + N^{-1/4}$ are chosen to decrease with N in a way that guarantees optimal asymptotic performance in the standard Ramsey interferometry protocol in the presence of uncorrelated dephasing [67, 68, 69]. The important characteristic of this state, which in the end allows for the optimal phase estimation, is its first and second moments:

$$\langle\sigma_x^{(n)}\rangle \simeq 1, \qquad \langle\sigma_y^{(n)}\rangle = 0, \qquad \langle\sigma_\alpha^{(n)}\sigma_\alpha^{(n)}\rangle = 1 \tag{12}$$

$$\langle\sigma_x^{(i)}\sigma_x^{(j)}\rangle \simeq 1, \quad \langle\sigma_y^{(i)}\sigma_y^{(j)}\rangle \simeq \frac{-1}{N}, \quad \langle\sigma_x^{(i)}\sigma_y^{(j)}\rangle \simeq 0, \tag{13}$$

for $i \neq j$. Throughout this paper we use the symbol $\simeq$ to mean that such approximation correctly predicts first-order asymptotic behavior of QFI or precision in the limit $N \to \infty$.

After the state is evolved in parallel through channel $\Lambda_\theta^{(N)}$, the value of θ is inferred based on the measurement of the J_y observable on the output state $\rho_\theta^{(N)} = \Lambda_\theta^{(N)}(\rho^{(N)})$. We may assess the estimation variance of this procedure via the standard linear error propagation formula:

$$\hat{\theta} = \frac{J_y}{\partial_\theta\langle J_y\rangle}, \quad \mathrm{Var}(\hat{\theta}) = \frac{\mathrm{Var}(J_y)}{|\partial_\theta\langle J_y\rangle|^2}, \tag{14}$$

where $\hat{\theta}$ is the operator representing the local unbiased estimator, whose eigenvalues are the values of θ to be estimated.

Let us analyze the performance of the above protocol using the SS probe state and J_y measurement for the correlated noise. We will use standard Heisenberg picture methods to compute the first and second moments of the J_y observable by evolving the operators back through the channel and then compute the expectation values on the initial state (11) [68]. Without loss of generality, we assume the estimation is performed around $\theta = 0$. In order to compute the estimation variance, we need to compute the following:

$$\partial_\theta\langle J_y\rangle = \langle J_x\rangle = \frac{1}{2}\sum_{i=1}^{N}\langle\sigma_x^{(i)}\rangle, \tag{15}$$

$$\mathrm{Var}(J_y) = \frac{1}{4}\sum_{i,j=1}^{N}\langle\sigma_y^{(i)}\sigma_y^{(j)}\rangle. \tag{16}$$

For compactness of notation, in what follows all operator expectation values, $\langle\hat{A}\rangle$, are understood to be performed on the output state $\rho_\theta^{(N)}$, while when we write $\langle f(\vec{\varphi})\rangle$ with $f(\vec{\varphi})$ being some function of classical random variable $\vec{\varphi}$, we understand that this represents averaging with respect to Gaussian probability distribution (4).

With the help of SS properties (11) the relevant moments of Pauli matrices can be expressed in terms of statistical properties of fluctuating phases

$$\langle\sigma_x^{(n)}\rangle \simeq \langle\cos\varphi_n\rangle = e^{-\sigma^2/2} = \eta \tag{17}$$

$$\langle\sigma_y^{(i)}\sigma_y^{(j)}\rangle \simeq \langle\sin\varphi_i\sin\varphi_j\rangle - \frac{1}{N}\langle\cos\varphi_i\cos\varphi_j\rangle, \tag{18}$$

for $i \neq j$, where

$$\langle\sin\varphi_i\sin\varphi_j\rangle = e^{-\sigma^2}\sinh\left(\sigma^2 c^{|i-j|}\right), \tag{19}$$

$$\langle\cos\varphi_i\cos\varphi_j\rangle = e^{-\sigma^2}\cosh\left(\sigma^2 c^{|i-j|}\right). \tag{20}$$

In (17) we have introduced $\eta = e^{-\sigma^2/2}$ that represents the effective shrinking factor of the Bloch

vector of a single qubit state under the dephasing process. We may now obtain the formula for the estimation variance, which for simplicity we write in the form valid in the asymptotic $N \to \infty$ regime (assuming $|c| < 1$ so that correlations die exponentially):

$$\mathrm{Var}(\hat{\theta})_{\mathrm{SS}} \simeq \frac{1-\eta^2+2\eta^2\sum_{k=1}^{\infty}\sinh(\sigma^2 c^k)}{N\eta^2}. \quad (21)$$

Note that for the uncorrelated dephasing case $c = 0$, we recover the well-known result that

$$\mathrm{Var}(\hat{\theta}) \simeq \frac{1-\eta^2}{N\eta^2}, \quad (22)$$

which saturates the fundamental bound [20, 21], proving that the strategy is asymptotically optimal. Similarly, we can compute the variance for the product probe state by setting $\langle \sigma_y^{(i)}\sigma_y^{(j)}\rangle = 0$ instead to obtain:

$$\begin{aligned}\mathrm{Var}(\hat{\theta})_{\mathrm{product}} &\simeq \frac{1+2\eta^2\sum_{k=1}^{\infty}\sinh(\sigma^2 c^k)}{N\eta^2} \quad (23)\\ &= \mathrm{Var}(\hat{\theta})_{\mathrm{SS}} + \frac{1}{N}.\end{aligned}$$

The improvement due to squeezing by an additive factor $1/N$ can be generalized for other estimation schemes and noise correlations, and we refer the reader to Appendix D for the general proof.

In the next section, we will provide a bound based on the classical simulation idea that will allow us to see if there is space for improvement over the spin-squeezed state protocol in the presence of correlations.

4 Classical simulation bound

To assess the precision of estimation, we now focus on deriving upper bounds on QFI with correlated noise using the *classical simulation (CS) method* [21, 70]. We call a parametrized quantum channel classically simulable if it admits a decomposition into a convex mixture of θ-independent channels with θ-dependent classical weights

$$\Lambda_\theta(\rho) = \int \mathrm{d}p_\theta(x)\tilde{\Lambda}_x(\rho). \quad (24)$$

This decomposition allows us to split the estimation error into quantum error—due to the indistinguishability of channels $\{\tilde{\Lambda}_x\}$, and a classical error—caused by nondeterministic classical mixing with probability distribution $p_\theta(x)$. By neglecting quantum error, we can bound the channel QFI (optimize QFI over all possible input states) by the classical Fisher information (CFI) of the distribution $p_\theta(x)$,

$$\mathcal{F}_Q(\Lambda_\theta) \le \mathcal{F}_{\mathrm{cl}}[p_\theta(x)] = \int \mathrm{d}x\, \frac{1}{p_\theta(x)}\left(\frac{\mathrm{d}p_\theta(x)}{\mathrm{d}\theta}\right)^2. \quad (25)$$

This bound can be easily applied for model (6) if we rewrite the action of the channel as:

$$\Lambda_\theta^{(N)}(\cdot) = \int \mathrm{d}p_\theta(\vec{\xi})\left(\bigotimes_{n=1}^{N} U_{\xi_n}\right)(\cdot)\left(\bigotimes_{n=1}^{N} U_{\xi_n}\right)^\dagger, \quad (26)$$

where

$$p_\theta(\vec{\xi}) = p(\vec{\theta}-\vec{\xi}), \quad (27)$$

and $\vec{\theta} = [\theta, \ldots, \theta]^T$. We can now compute the CFI for the classical Gaussian statistical model $p_\theta(\vec{\xi})$, making use of the fact that it represents a Markovian process, we can express the CFI in terms of CFIs of the marginal distribution of neighboring phases and single-phase distribution [59, 71]:

$$\begin{aligned}\mathcal{F}_{cl}(\vec{\xi}) &= (N-1)\mathcal{F}_{cl}(\xi_2,\xi_1) - (N-2)\mathcal{F}_{cl}(\xi_1) \simeq\\ &\simeq N[\mathcal{F}_{cl}(\xi_2,\xi_1) - \mathcal{F}_{cl}(\xi_1)]. \quad (28)\end{aligned}$$

For our model we get

$$\mathcal{F}_{cl}(\varphi_2,\varphi_1) = \frac{2}{1+c}\sigma^{-2}, \quad \mathcal{F}_{cl}(\varphi_1) = \sigma^{-2}, \quad (29)$$

which finally leads to the CS bound [72]:

$$\mathcal{F}_Q^{(N)} \le N\sigma^{-2}\frac{1-c}{1+c}. \quad (30)$$

Unfortunately, this bound is not tight, even for the uncorrelated case $c = 0$—comparing with (22), we see that the bound on QFI should be $F_Q^{(N)} \le \frac{N\eta^2}{1-\eta^2} = N/(e^{\sigma^2}-1)$, which is strictly tighter than N/σ^2.

To solve this problem, we propose a tighter, refined bound, based on decomposition of the Gaussian noise into uncorrelated and correlated parts:

$$\mathcal{N}(\theta,\Sigma) \sim \mathcal{N}(q\theta,\lambda\mathbb{1}) + \mathcal{N}((1-q)\theta,\Sigma-\lambda\mathbb{1}), \quad (31)$$

$$\mathcal{F}_Q^{(N)} \le q^2\mathcal{F}_{\mathrm{uncorrelated}} + (1-q)^2\mathcal{F}_{\mathrm{correlated}}, \quad (32)$$

$$\mathcal{F}_{\mathrm{uncorrelated}} = \mathcal{F}_Q^{(N)}\Big|_{c=0,\eta=\eta(\lambda)} = \frac{N\eta(\lambda)^2}{1-\eta(\lambda)^2}, \quad (33)$$

$$\mathcal{F}_{\mathrm{correlated}} = \mathcal{F}_{\mathrm{cl}}(\mathcal{N}(\theta,\Sigma-\lambda\mathbb{1})), \quad (34)$$

where λ is the smallest eigenvalue of Σ, so that $\Sigma - \lambda\mathbb{1}$ is semi-definite positive, therefore a valid covariance matrix, $\eta(\lambda)^2 = e^{-\lambda}$ is the strength of uncorrelated noise and $q \in [0,1]$ controls splitting of θ. Assuming $c \geq 0$, and optimizing over q, we obtain:

$$\mathcal{F}_Q^{(N)} \leq (\mathcal{F}_{\text{uncorrelated}}^{-1} + \mathcal{F}_{\text{correlated}}^{-1})^{-1}, \tag{35}$$

where (see Appendix B for more details)

$$\mathcal{F}_{\text{uncorrelated}} = \frac{N}{e^{\lambda} - 1} = \frac{N}{\exp\left(\sigma^2 \frac{1-c}{1+c}\right) - 1}, \tag{36}$$

$$\mathcal{F}_{\text{correlated}} \simeq N \frac{1-c^2}{4c\sigma^2}. \tag{37}$$

For $c < 0$, above method gives divergent $\mathcal{F}_{\text{correlated}} = \infty$, so the bound (35) simplifies to $\mathcal{F}_Q^{(N)} \leq N/(e^{\lambda} - 1)$, where $\lambda = \sigma^2 \frac{1+c}{1-c}$. Finally, the refined CS bound reads:

$$\frac{F_Q^{(N)}}{N} \leq \begin{cases} \left[\exp\left(\sigma^2 \frac{1-c}{1+c}\right) + \sigma^2 \frac{4c}{1-c^2} - 1\right]^{-1} & c > 0, \\ \left[\exp\left(\sigma^2 \frac{1+c}{1-c}\right) - 1\right]^{-1} & c \leq 0. \end{cases} \tag{38}$$

Comparison of CS bounds with respect to known achievable precision (21) is presented in Fig. 2. We observe significant improvement of the refined CS bound (38) over the standard bound (30) for weak correlations. Moreover, the analytical form of the bound enables a clear distinction between correlated and uncorrelated noise scenarios, thereby providing valuable insights into the effects of noise correlations.

We see that for positive correlations $c \geq 0$, spin-squeezed states perform extremely well, and the bound indicates that there is not much space for further improvement. On the other hand, we see that for negative correlations, $c < 0$, the gap between the spin-squeezed state protocol and the bound is larger, giving hope for the existence of better protocols.

Generally, we can derive the refined CS bound for any dephasing model, without assuming Gaussianity or the Markov property. If we find decomposition of noise into several N-variate random variables $\mathcal{R}_k$

$$\vec{\varphi} \sim \sum_{k=1}^{n} \vec{\mathcal{R}}_k, \quad \mathcal{F}_Q^{(N)} \leq \left(\sum_{k=1}^{n} \mathcal{F}(\vec{\theta} + \vec{\mathcal{R}}_k)^{-1}\right)^{-1} \tag{39}$$

where $\mathcal{F}$ is the FI of classical simulation, which is equal to QFI for the uncorrelated variables.

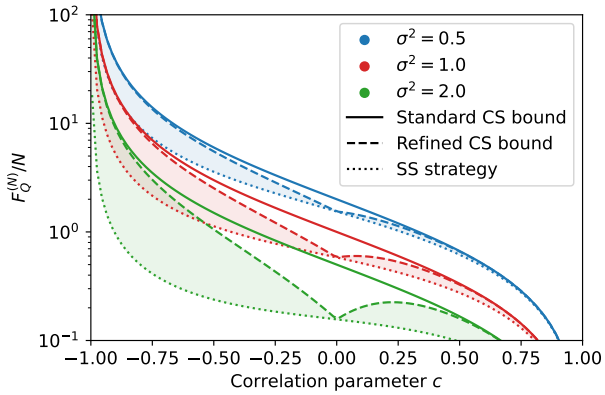

Figure 2: Comparison of standard CS bound (30)—solid lines—and refined CS bound (38)—dashed lines—to precision of SS probe state strategy with J_y measurement (21)—dotted lines—for Markovian Gaussian noise model (4). The actual QFI lies inside the shaded regions. We see that the refined bound is tight at $c = 0$ and is significantly tighter than the standard bound for weakly correlated noise. Moreover, for strong positive correlations, both bounds and SS strategy yield similar FI, coinciding in the limit $c \to 1$.

On the level of probability distributions condition (39) can be written as

$$p(\vec{\varphi}) = p(\vec{\mathcal{R}}_1) * p(\vec{\mathcal{R}}_2) * \cdots * p(\vec{\mathcal{R}}_n) \tag{40}$$

where $*$ is the convolution operator. For many cases, it is easy to decompose $p(\vec{\varphi})$ in this way by working on the Fourier transform of distributions, where convolution is mapped to multiplication. For Gaussian variables, this condition is simply that the sum of covariance matrices of $\vec{\mathcal{R}}_k$ is Σ.

5 Optimized protocols using tensor network approach

There are mainly two well-known approaches for computing QFI numerically. The first one, the minimization over purifications, has some serious drawbacks [51]; therefore, we follow the *iterative see-saw (ISS)* approach, which is far more convenient. Let us consider the *pre-QFI function*

$$\mathcal{F}(\rho, L) = 2\mathrm{Tr}(\dot{\rho}_\theta L) - \mathrm{Tr}(\rho_\theta L^2), \quad \rho_\theta = \Lambda_\theta(\rho), \tag{41}$$

where L is a Hermitian operator. The quantum Fisher information optimized over all input states ρ can be obtained as $\mathcal{F}_Q = \max_{\rho,L} \mathcal{F}(\rho, L)$.

The double maximization of the ISS protocol is an iterative process that goes as follows. Firstly, perform the maximization of $\mathcal{F}(\rho, L)$ over L for

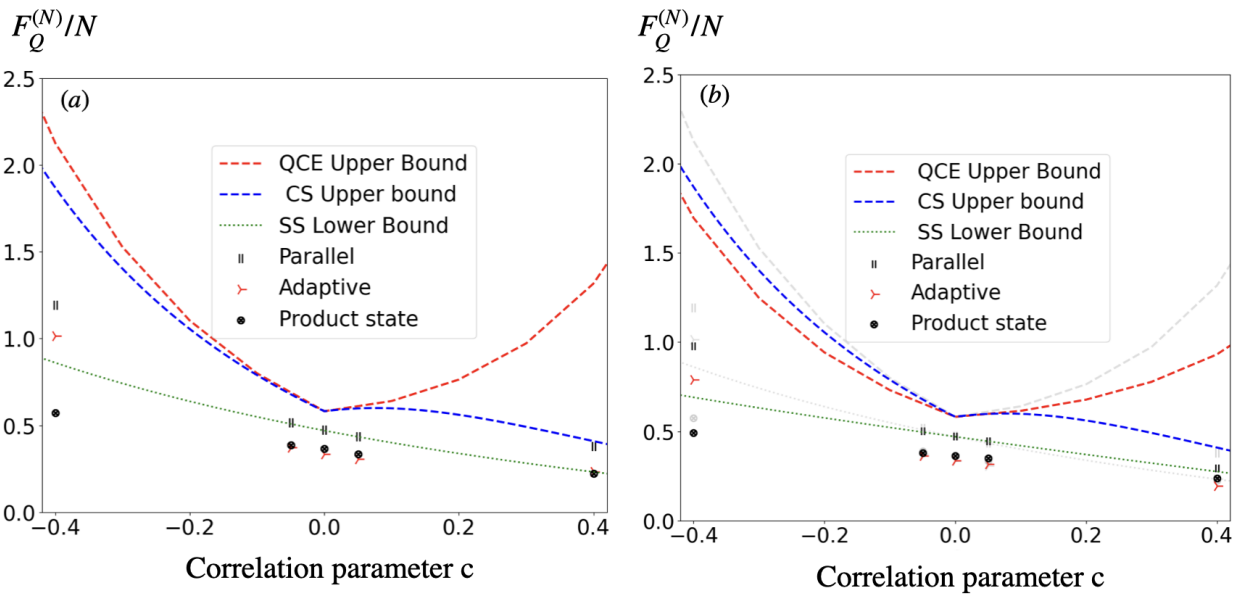

Figure 3: The dashed lines indicate the asymptotic upper bounds of the quantum Fisher information per channel, $\lim_{N\to\infty} \mathcal{F}_Q^{(N)}/N$, as a function of the correlation parameter c. **(a)** The left panel contains the binary phase, i.e., $M = 2$ and **(b)** the right panel demonstrates $M = 4$. The red curve represents the upper bound obtained from the QCE method with the Rouwenhorst approximation, and the blue curve is the tighter upper bound obtained by the classical simulation bound (38) for the actual Gaussian noise model. The dotted green line denotes the lower bound for the approximate model with an SS state as the initial probe state at $N = 30$. The scattered points correspond to the computed values of $\mathcal{F}_Q^{(N)}/N$ with $N = 30$ for the discretized model, obtained via tensor network optimization. For the parallel strategy, the bond dimension of the input state is considered to be 4 and 1, which correspond to entangled (marked as ||) and product states (marked as •), respectively. For the adaptive strategy, we consider the ancilla dimension to be 3. We also plot results for $M = 2$ on the right panel with grayed lines to better appreciate the effect of more refined phase discretization. Here $\sigma^2 = 1$.

an arbitrary input state (educated guess) $\rho = \rho^0$, to obtain L^0. Then for the aforementioned L^0, again maximize the function with respect to ρ to obtain ρ^1. One needs to repeat this procedure until the function $\mathcal{F}(\rho, L)$ converges to some $\mathcal{F}(\rho^i, L^i)$. Both steps of optimization boil down to solving a simple convex optimization problem, either an unconstrained quadratic in the case of optimization with respect to L, or a semi-definite programming problem with $\rho \geq 0, \mathrm{Tr}(\rho) = 1$ constraints in the latter case.

For a single-channel application, the aforementioned method can accurately determine the ideal probe condition for any metrological protocol. For multiple uses of the channel, if all of them are uncorrelated, one can use the ISS method with Λ_θ substituted by $\Lambda_\theta^{\otimes N}$. The mathematical tool used to handle the adaptive protocol is the quantum comb [63, 73]. For the correlated channel estimation, the $N-$partite quantum channel $\Lambda_\theta^{(N)}$ does not follow product structure $\Lambda_\theta^{(N)} \neq \Lambda_\theta^{\otimes N}$. The optimization over combs becomes inefficient for large N, as the size of the optimized comb grows exponentially with N. To avoid this, one can efficiently represent a quantum comb with a tensor network [52].

To model classical Markovian noise we introduce auxillary quantum environment with orthogonal basis indexed by Markov chain state-space $\{|\phi\rangle\}$ and a quantum channel defined with Kraus operators indexed by pairs of basis vectors:

$$K(\phi_{\mathrm{IN}}, \phi_{\mathrm{OUT}}) = \sqrt{p(\phi_{\mathrm{OUT}}|\phi_{\mathrm{IN}})} U_{\phi_{\mathrm{OUT}}} \otimes |\phi_{\mathrm{OUT}}\rangle\langle\phi_{\mathrm{IN}}|, \tag{42}$$

where $p(\phi_{\mathrm{OUT}}|\phi_{\mathrm{IN}})$ is the transition probability distribution of the Markov chain. The state of the auxiliary system transfers the state of the Markov chain, while the probe system experiences random unitary rotation with corresponding probabilities. For implementing this approach numerically, we need a discretized version of our continuous noise model, which closely approximates the stochastic correlations while benefiting from a finite state-space $\{\phi_k\}$ with $k = 1, \ldots, M$. From

a broad family of potential discretizations, we choose the *Rouwenhorst process* [74]. The transition probability distribution is defined as coefficients of a polynomial:

$$\sum_{i=1}^{M} p^{(c)}(\phi_i|\phi_j)t^{i-1} = 2^{1-M} \tag{43}$$
$$[(1+c)+(1-c)\,t]^{M-j}\,[(1-c)+(1+c)\,t]^{j-1}\,.$$

These transition probabilities satisfy

$$\sum_{k=1}^{M} p^{(c_1)}(\phi_i|\phi_k)p^{(c_2)}(\phi_k|\phi_j) = p^{(c_1\cdot c_2)}(\phi_i|\phi_j). \tag{44}$$

The condition (44) guarantees that if $\langle\varphi_k\rangle, \mathrm{Var}(\varphi_k)$ and $\langle\varphi_k\varphi_{k+1}\rangle$ for the Rouwenhorst process and the continuous Gaussian process are equal, then the whole covariance matrices are identical. The stationary distribution of the Rouwenhorst process is a binomial distribution $p(\phi_k) = 2^{1-M}\binom{M-1}{k-1}$, and therefore, due to De Moivre-Laplace theorem the correct choice of states $\{\phi_k\}$ are equally spaced in an interval symmetric around 0 of width dependent on the noise strength—in our case we numerically find the width such that $\eta = \langle\cos\varphi\rangle$ for stationary distributed φ. The equality of $\langle\varphi_k\varphi_{k+1}\rangle$ holds when the correlation parameter c is identical in both the Gaussian and Rouwenhorst processes. With matched first and second moments, we can approximate the Gaussian noise with the derived discretisation, and this approximation is especially good for moderate values of c or large M.

Using the obtained Kraus operators (42), we determine the optimal schemes for both parallel and adaptive scenarios using the functions `iss_tnet_adaptive_qfi` and `iss_tnet_parallel_qfi`, from the QMetro++ Python optimization package [75]. These functions are efficient even for a moderately large ($N \approx 30$) number of channels thanks to tensor network methods. These tensor network decompositions assume a limited available memory size for adaptive protocols and limited bond dimension of the input entangled state for parallel protocols. The results for $M = 2$ and $M = 4$ are shown in Fig. 3. The bond dimension of MPS in parallel optimization was fixed at 4 and the memory size in adaptive optimization was set to 3, which allowed for efficient numerical optimization in reasonable time up to the number of channels used $N \approx 30$.

Additionally, we compute fundamental upper bounds for QFI using the method `ad_asym_bounds_correlated` from the QMetro++ package. These bounds are based on the *quantum comb extension* (QCE) technique, in which the QFI of a more powerful strategy, in which control comb may affect normally inaccessible environments, is used as an upper bound for the QFI of normal adaptive schemes. The bounds are valid both for parallel and adaptive strategies with unlimited memory and MPS bond dimension, see [52] for more details. For both positive and negative correlations, the bond dimensions of the probe state and the corresponding SLD operators are equal to 4, exceeding that of the adaptive strategy. Note that the bounds are asymptotically valid for $N \to \infty$, which explains a gap between the bounds and the performance of the actual protocols for $c = 0$, which will close if one increases N further.

A detailed numerical investigation indicates that for both moderately positive, negative and also for uncorrelated scenarios, (i.e., approximately, $|c| \leq 0.5$) the difference in the computed Fisher information between discretizations with $M = 4$ and $M = 5$ phases is negligible for all practical purposes (see Appendix C), indicating that $M = 4$ discrete phases are sufficient to faithfully approximate the continuous noise. Although increasing the value of M yields a finer approximation of the continuous noise, the improvement is not substantial enough to affect the determination of the optimal strategy for the protocol. Therefore, to ensure computational efficiency while maintaining sufficient accuracy, we adopted $M = 4$ throughout the numerical simulations.

Our systematic analysis reveals that although the CS method is generally considered weaker than the QCE approach [52] for estimating the upper bound of the Fisher information, in the presence of positive correlations, the CS method provides a tighter bound. Notably, both bounds coincide near $c = 0$. We determine the optimal strategies that saturate these bounds using SS states and matrix product states with a bond dimension of 4. As shown in Fig. 3, the parallel strategy proves to be more efficient than the adaptive one (with the assumed ancillary space

dimension) in reaching the asymptotic limit—it appears that in order to reach the asymptotic performance in the adaptive paradigm, the size of the ancillary system would need to grow with the number of channel uses and hence it is much more efficient to look for optimal strategies using parallel strategies involving MPS states.

Indeed, for both positive and negative correlations, MPS as probe states outperform the SS state strategy, with the advantage being particularly pronounced for $c < 0$. Increasing the bond dimension is expected to further enhance performance; however, for the uncorrelated and positively correlated case $c > 0$, this advantage is expected to fade away asymptotically when $N \to \infty$. In contrast, for $c < 0$, the advantage of the MPS approach over the SS strategy is substantial, and already for finite $N \approx 30$ provides a ratio F_Q/N larger than the asymptotic ratio $\lim_{N\to\infty} F_Q/N$ achievable with SS strategy

Moreover, one might wonder if including measurements of higher-order observables in the SS strategy could offer comparable improvement. We have verified that this advantage may only be observed in strong noise and strong negative correlation regimes and will not affect the performance for the moderate noise strength $\sigma^2 = 1$ discussed above—see Appendix D for detailed discussion.

6 Discussion

In this work, we have investigated a metrological frequency estimation protocol in which phase-encoding quantum channels exhibit noise correlations.

The general tools to optimize metrological protocols and derive fundamental bounds for correlated cases have been proposed in Ref. [51] and Ref. [52], respectively. The toy model involving binary correlated dephasing, for which random rotations angles φ_n take only two possible values, has been studied in both aforementioned references as an illustration of the introduced techniques.

However, the generalization to more realistic models in which φ_n are given by a continuous-valued stochastic process remains a non-trivial task. The methods derived in Refs. [51,52] cannot be directly applied in this case, as doing so would require the use of intractable combs with infinite memory to properly model noise correlations.

In this work, we overcome this difficulty and, for the first time, comprehensively study metrological scenarios involving correlated dephasing governed by a realistic Gaussian Markov process.

To derive fundamental metrological bounds, we use the CS technique, which is applicable directly to continuous-variable processes. We generalize a known uncorrelated bound [21] to cases involving correlations. We further tighten the obtained bound by incorporating the novel idea of dividing the noise into correlated and uncorrelated parts and using an appropriate classical simulation for each part independently.

Furthermore, we analyze the performance of squeezing-based metrological protocols—such protocols have so far been studied for uncorrelated noise only. We show that squeezing remains a valuable metrological resource also in the presence of correlations. An interesting difference between uncorrelated and correlated cases is that higher spin moments may be an additional source of information in the latter case, as discussed in Appendix D.

Finally, we show how to approximate a continuous noise model with a discretized model using the Rouwenhorst method. This allows to apply the techniques developed in Refs. [51, 52] for a comparison.

7 Codes and data availability

The computer codes for generating numerical data used in this paper are available at [76].

Author Contribution Statement

S.G. and A.K. contributed equally to this work. All authors contributed to the conceptualization of the research, development of the theoretical framework, analysis of the results, and preparation of the manuscript. All authors reviewed and approved the final version.

ACKNOWLEDGMENTS

S.G. thanks Arpan Das for fruitful discussions and Piotr Dulian for the support in running the numerics with the help of the QMetro++ package. S.K. is a recipient of the Foundation for

Polish Science START 2025 scholarship. This work was supported by National Science Center (Poland) grant No.2020/37/B/ST2/02134.

A Discretization of a time-continuous frequency estimation model with Ornstein-Uhlenbeck fluctuations

We focus on detailed description of experimentally relevant example of time-varying, correlated process, the *Ornstein-Uhlenbeck (OU) model* [56, 57, 58, 59, 60], which is constructed with independent Gaussian increments:

$$\mathrm{d}\omega(t) = \alpha(\omega - \omega(t))\mathrm{d}t + \beta \mathrm{d}W(t), \tag{45}$$

where $\alpha, \beta > 0$, $W(t)$ is the Wiener process, and ω is the mean value. The mean-revertability, critical for estimation protocol, is introduced via drift coefficient α, which controls the strength of correlations. By integrating the process from time $t_n = (n-1)\delta t$ to $t_{n+1} = n\delta t$, we obtain:

$$\varphi_n = \int_{t_n}^{t_{n+1}} \omega(t)\mathrm{d}t, \quad \langle \varphi_n \rangle = \delta t \omega, \tag{46}$$

$$\mathrm{Var}(\varphi_n) = \frac{\beta^2}{\alpha^3}(e^{-\alpha\delta t} + \alpha\delta t - 1) \approx \frac{\beta^2}{2\alpha}\delta t^2, \tag{47}$$

$$\mathrm{Cov}(\varphi_i, \varphi_j) = \frac{2\beta^2}{\alpha^3}\sinh^2\left(\frac{\alpha\delta t}{2}\right) e^{-\alpha\delta t|i-j|} \approx \tag{48}$$

$$\approx \frac{\beta^2}{2\alpha}\delta t^2 e^{-\alpha\delta t|i-j|}, \quad i \neq j,$$

where the approximations are valid for $\alpha\delta t \approx 0$—in this regime the covariance matrix is identical to model (4) for $c = e^{-\alpha\delta t} \approx 1$. Whenever $\alpha\delta \approx 0$, $\vec{\varphi}$ does not satisfy the Markov property (the integral is not sufficient statistics for deriving the conditional probability distribution with the Markov property), and the covariance matrix differs from the Markovian model by a factor proportional to the identity matrix. In fact, all results of this paper may be used for this model, either directly (SS strategy and CS bound with changed values of η and λ) or with slight modification (using a hidden Markov model instead of a Markov chain for numerical analysis).

Let us also translate the CS bound (30) for the OU model estimation with total sensing time $T = N\delta t$ being the limited resource, instead of the number of qubits N:

$$\mathrm{Var}(\hat{\omega}) \geq \frac{\sigma^2}{N}\frac{1+c}{1-c}\left|\frac{\partial\omega}{\partial\theta}\right|^2 = \frac{\delta t \beta^2}{2\alpha T}\frac{1+e^{-\alpha\delta t}}{1-e^{-\alpha\delta t}} \geq \frac{\beta^2}{\alpha^2}T^{-1}, \tag{49}$$

where the optimal estimation is achieved for $\delta \to 0$ and $N \to \infty$. Moreover, the bound can be saturated by estimator (14) for the product probe state. Although this limit is not physical, as it requires qubit manipulations in infinitesimal time, it shows that performing more measurements is beneficial, even if the outcomes are highly correlated.

B CFI of correlated part of Markovian Gaussian process

We derive Eq. (37) for the CFI of correlated part of Gaussian noise. As $\mathcal{N}(\vec{\theta}, \Sigma - \lambda\mathbb{1})$ is no longer a Markov chain, we have to compute its CFI via an explicit result for multivariate Gaussian variables [77]:

$$\mathcal{F}_{\mathrm{cl}}(\mathcal{N}(\vec{\theta}, \Sigma - \lambda\mathbb{1})) = \sum_{i,j=1}^{N}(\Sigma - \lambda\mathbb{1})^{-1}_{ij}, \tag{50}$$

which requires inversion of a large matrix. This can be performed for our case, as there exists a known asymptotic eigendecomposition of Σ [78]:

$$\Sigma = VDV^T, \quad V_{ij} \simeq \sqrt{\frac{2}{N+1}}\sin\left(\frac{ij}{N+1}\pi\right), \tag{51}$$

$$D_{ij} \simeq \delta_{ij}\sigma^2\frac{1-c^2}{1+c^2-2c\cos\left(\frac{i\pi}{N+1}\right)}, \quad \lambda = \sigma^2\frac{1-c}{1+c}, \tag{52}$$

for $c \geq 0$ and

$$V_{ij} \simeq \sqrt{\frac{2}{N+1}}\sin\left(\frac{ij}{N+1}\pi\right)(-1)^{i+j}, \tag{53}$$

$$D_{ij} \simeq \delta_{ij}\sigma^2\frac{1-c^2}{1+c^2-2c\cos\left(\frac{i\pi}{N+1}\right)}, \quad \lambda = \sigma^2\frac{1+c}{1-c}, \tag{54}$$

for $c < 0$. Let us note that we chose λ to be less than the smallest eigenvalue of Σ, but converging to it in the limit $N \to \infty$, which still provides a valid bound for finite N and does not change the asymptotic bound, but ensures that $\Sigma - \lambda\mathbb{1}$

is invertible. Let us assume $c \geq 0$ and use the eigendecomposition to write:

$$(\Sigma - \lambda \mathbb{1})^{-1} = V(D - \lambda \mathbb{1})^{-1} V^T, \tag{55}$$

and therefore:

$$\mathcal{F}_{\text{correlated}} = \sum_{i,j,k=1}^{N} \frac{V_{ik} V_{jk}}{D_{kk} - \lambda} \simeq \tag{56}$$

$$\simeq \frac{2}{N\sigma^2} \sum_{i,j,k=1}^{N} \frac{\sin\left(\frac{ik}{N+1}\pi\right) \sin\left(\frac{jk}{N+1}\pi\right)}{\frac{1-c^2}{1+c^2-2c\cos(k\pi/(N+1))} - \frac{1-c}{1+c}}$$

First, let us compute the sum:

$$\sum_{i=1}^{N} \sin\left(\frac{ik}{N+1}\pi\right) \simeq N \int_0^1 \sin(k\pi x) \mathrm{d}x =$$

$$= \begin{cases} \frac{2N}{k\pi} & \text{if } k \text{ is odd,} \\ 0 & \text{if } k \text{ is even,} \end{cases} \tag{57}$$

which, when substituted back, yields:

$$\mathcal{F}_{\text{correlated}} \simeq \frac{8N}{\pi^2\sigma^2} \sum_{\text{odd } k}^{N} \frac{k^{-2}}{\frac{1-c^2}{1+c^2-2c\cos(k\pi/(N+1))} - \frac{1-c}{1+c}}. \tag{58}$$

Even though for $k \approx N$ the denominator approaches 0, the rapidly diminishing numerator k^{-2} allows us to neglect this part of the sum, and assume that $\cos(k\pi/(N+1)) \simeq 1$. This may seem overly hand-wavy, but such an assumption, in fact, correctly predicts the asymptotic behavior. We continue with this assumption to obtain:

$$\mathcal{F}_{\text{correlated}} \simeq \frac{8N}{\pi^2\sigma^2} \sum_{\text{odd } k}^{N} \frac{k^{-2}}{\frac{1+c}{1-c} - \frac{1-c}{1+c}} =$$

$$= \frac{8N}{\pi^2\sigma^2} \frac{1-c^2}{4c} \sum_{\text{odd } k}^{N} k^{-2} \simeq$$

$$\simeq \frac{8N}{\pi^2\sigma^2} \frac{1-c^2}{4c} \frac{\pi^2}{8} = N \frac{1-c^2}{4c\sigma^2}. \tag{59}$$

The above argument fails for $c < 0$, as the denominator approaches 0 for $k = 1$, yielding CFI diverging to ∞.

C How many phases are sufficient to approximate Gaussian noise?

A detailed numerical investigation of the Rouwenhorst process-driven dephasing indicates that for both moderate positive and negative correlations as well as for the uncorrelated case, the difference in the computed Fisher information between discretizations with $M = 4$ and $M = 5$ phases is negligible for all practical purposes (see Fig. 4). Although increasing the value of M yields a finer approximation of the continuous noise, the improvement is not substantial enough to affect the determination of the optimal strategy for the protocol. Therefore, to ensure computational efficiency while maintaining sufficient accuracy, we adopted $M = 4$ throughout the numerical simulations presented in the main text.

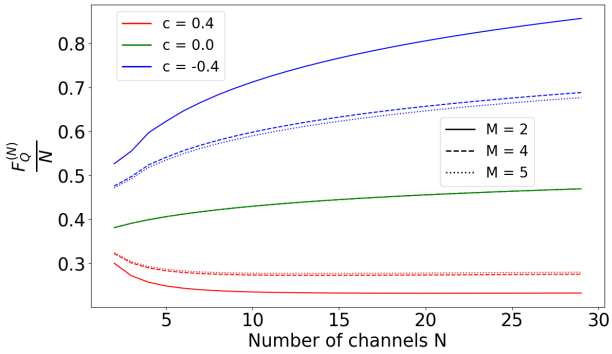

Figure 4: Fisher information per channel $F_Q^{(N)}/N$ with the number of channel uses N with SS probe state.

We should note, however, that irrespective of how many finite discrete phases one chooses, the resulting model will not be able to reconstruct properties of the continuous Gaussian model for strong enough correlations $|c| \approx 1$. In particular, for any discretized model, when correlations are strong enough, and we use enough probes, we may estimate the phase better than the phase noise discretization step, and hence be able to separate noise from the signal; see more quantitative analysis at the end of Appendix D.

D Estimation protocol with higher-order moment measurements

Previously, we have discussed an estimation protocol with SS state and J_y measurement, which is optimal for uncorrelated noise. To generalize this protocol we introduce a *multi-observable estimator* based on measured observables $\vec{X}$ with coefficients $\vec{\xi}$normalized to satisfy the local unbi-

asedness condition:

$$\hat{\theta} = \frac{\vec{\xi}^T \vec{X}}{\vec{\xi}^T \partial_\theta \langle \vec{X} \rangle}, \qquad \mathrm{Var}(\hat{\theta}) = \frac{\vec{\xi}^T \mathrm{VAR}(\vec{X}) \vec{\xi}}{|\vec{\xi}^T \partial_\theta \langle \vec{X} \rangle|^2}, \quad (60)$$

$$\mathrm{VAR}(\vec{X})_{mn} = \frac{1}{2}\langle X_m X_n + X_n X_m \rangle - \langle X_m \rangle \langle X_n \rangle. \quad (61)$$

Minimizing the variance over coefficients $\vec{\xi}$ yields the optimal estimator for $\vec{\xi} = \mathrm{VAR}(\vec{X})^{-1} \partial_\theta \langle \vec{X} \rangle$, with variance:

$$\mathrm{Var}(\hat{\theta}) = (\partial_\theta \langle \vec{X} \rangle^T \mathrm{VAR}(\vec{X})^{-1} \partial_\theta \langle \vec{X} \rangle)^{-1}. \quad (62)$$

For the optimal estimator, we should include as many observables as possible in the scheme, and as $\sigma_y^{(n)}$ are the informative local measurements, we consider observables which are polynomials in variables $\sigma_y^{(n)}$ for $n \in \{1, \cdots, N\}$. For the most general translationally invariant scheme, we define observables:

$$X_{t_1, \cdots, t_k} = \sum_{n=1}^{N-t_k} \sigma_y^{(n)} \sigma_y^{(n+t_1)} \cdots \sigma_y^{(n+t_k)}, \quad (63)$$

for t_i being any strictly increasing sequence of positive integers. Although the number of such possible sequences grows with N, we can introduce a finite cutoff limiting the number of allowed sequences $t_k \leq t_{\max}$, as increasing $t_{\max}$ has diminishing influence over the scheme. By including an observable with an empty index $X_\circ = 2J_y$, we see that this scheme includes the previous estimation protocol as a special case. The crucial difference is that J_y is only sensitive to the proportion of positive to negative spin measurement outcomes, and therefore neglects patterns (such as clustering or repulsion of identical measurement results). For the uncorrelated case, the proportion of outcomes is a sufficient statistic, but for the correlated case we need to include patterns to obtain the optimal estimator.

As $\langle \vec{\varphi} \rangle = \vec{0}$, only odd moments are sensitive to parameter θ, and moreover, odd moments are uncorrelated with even moments, thus making even moments unnecessary in the estimation scheme. For computing such moments, let us notice that SS states are Gaussian states, that is, spin operators can be described as components of a multivariate Gaussian distribution. As higher moments of Gaussian distributions can be described by first and second moments with Isserlis formula [79], with moments as in Eq. (12,13) we can write:

$$\left\langle \prod_{i=1}^{m} \sigma_x^{(k_i)} \prod_{j=1}^{n} \sigma_y^{(k_j)} \right\rangle_{\mathrm{SS}} \simeq$$

$$\simeq \begin{cases} \frac{n(n-1)}{2} \langle \sigma_x^{(k)} \rangle_{\mathrm{SS}}^m \langle \sigma_y^{(i)} \sigma_y^{(j)} \rangle_{\mathrm{SS}}^{n/2} & \text{if } n \text{ is even,} \\ 0 & \text{if } n \text{ is odd,} \end{cases} \simeq \quad (64)$$

$$\simeq \begin{cases} \frac{n(n-1)}{2} \left(\frac{-1}{N} \right)^{n/2} & \text{if } n \text{ is even,} \\ 0 & \text{if } n \text{ is odd,} \end{cases} \quad (65)$$

where all indices are pairwise different. After omitting terms of order N^{-2}, the only non-zero terms are for $n = 0$ or $n = 2$. For SS state rotated by phases $\vec{\varphi}$ we get:

$$\left\langle \prod_{i=1}^{n} \sigma_y^{(k_i)} \right\rangle = \left\langle \prod_{i=1}^{n} \left(\sigma_y^{(k_i)} \cos \varphi_{k_i} + \sigma_x^{(k_i)} \sin \varphi_{k_i} \right) \right\rangle_{\mathrm{SS}}$$

$$\simeq \prod_{i=1}^{n} \sin \varphi_{k_i} - \frac{1}{N} \sum_{i \neq j}^{n} \cos \varphi_{k_i} \cos \varphi_{k_j} \prod_{m \neq i,j}^{n} \sin \varphi_{k_m}. \quad (66)$$

Let us notice, that using Eq. (66) we can express the measurement covariance matrix as a sum of two terms:

$$\mathrm{VAR}(\vec{X}) \simeq K(\vec{X}) - \frac{1}{N} Q(\vec{X}), \quad (67)$$

where the leading term $K(\vec{X})$ is the covariance matrix calculated on non-squeezed, product probe state, and the correction term $Q(\vec{X})$ is due to spin-squeezing. We define $h(m)$ as number of Pauli matrices multiplied in each term of X_m. Let us note, that the leading order term in $\mathrm{VAR}(\vec{X})$ is of order N, so we are only interested in terms in $Q(\vec{X})$ of order N^2. This allows us to neglect $\sigma_y^2 = 1$ property in terms, where some of σ_y operators from X_m and X_n act on the same qubits, leading to:

$$Q(\vec{X})_{mn} \simeq \frac{\tilde{\partial}_\theta^2}{2} \sum_{i,j} \left\langle \prod_{k=1}^{h(m)} \sin \varphi_{i+t_k^{(m)}} \prod_{l=1}^{h(n)} \sin \varphi_{j+t_l^{(n)}} \right\rangle, \quad (68)$$

where $\tilde{\partial}_\theta^2$ is the second derivative with the restriction that both derivatives have to act on different functions. Now let us assume $\vec{\varphi}$ has exponentially vanishing correlations, so for example, processes with finite memory (Markov order). We first consider case when both derivatives act on the functions in the same product, say, without loss of

generality, it is the first one, to obtain the term:

$$\left|\sum_{i,j}\left\langle \frac{\tilde{\partial}_\theta^2}{2}\prod_{k=1}^{h(m)}\sin\varphi_{i+t_k^{(m)}}\prod_{l=1}^{h(n)}\sin\varphi_{j+t_l^{(n)}}\right\rangle\right| \leq \tag{69}$$

$$\leq \frac{h(m)^2}{2}\sum_{i,j}\left\langle \prod_{k=1}^{h(m)}\left|\sin\varphi_{i+t_k^{(m)}}\right|\prod_{l=1}^{h(n)}\left|\sin\varphi_{j+t_l^{(n)}}\right|\right\rangle \leq$$

$$\leq \frac{h(m)^2}{2}\sum_{i,j}\langle|\sin\varphi_i\sin\varphi_j|\rangle \simeq \frac{h(m)^2}{2}\sum_{i,j}A|c|^{|i-j|},$$

and due to exponential decay of correlations, the sum is of order N, and therefore is negligible. On the other hand, when both derivatives act on different products, we get:

$$\sum_{i,j}\left\langle \partial_\theta\left(\prod_{k=1}^{h(m)}\sin\varphi_{i+t_k^{(m)}}\right)\partial_\theta\left(\prod_{l=1}^{h(n)}\sin\varphi_{j+t_l^{(n)}}\right)\right\rangle =$$

$$= \sum_{i,j}\left\langle \partial_\theta\prod_{k=1}^{h(m)}\sin\varphi_{i+t_k^{(m)}}\right\rangle\left\langle \partial_\theta\prod_{l=1}^{h(n)}\sin\varphi_{j+t_l^{(n)}}\right\rangle, \tag{70}$$

as for $|i-j| \gg 1$ both products become uncorrelated. In conclusion, for our noise model we can take $Q(\vec{X}) \simeq \partial_\theta\langle\vec{X}\rangle\partial_\theta\langle\vec{X}\rangle^T$. We can therefore simplify Eq. (62) by inverting the covariance matrix using the Sherman-Morrison formula [80] and obtain:

$$\mathrm{Var}(\hat{\theta}) \simeq (\partial_\theta\langle\vec{X}\rangle^T K(\vec{X})^{-1}\partial_\theta\langle\vec{X}\rangle)^{-1} - \frac{1}{N}. \tag{71}$$

We see a $-1/N$ correction to the estimator variance with SS state probe state as compared to product probe state, independently on the observables vector $\vec{X}$. These results allow for significant simplification of further computation, removing all quantum correlations from the measurement optimization problem, and allow us to directly use some results from classical estimation theory. For example, if $\vec{\varphi}$ is multivariate Gaussian with small enough variances, we can use the approximation $\sin\varphi_k \approx \varphi_k$ during computation of moments. Under this assumption, higher-order moments don't improve the estimation scheme, as the first-order moment estimator saturates asymptotically the CR bound. Therefore, when dealing with Gaussian noise, we should expect noticeable improvement only for strong noise. Moreover, our numerical investigations show that the significant gain is obtained for $\sigma^2 \gg 1$ and $c \ll 0$.

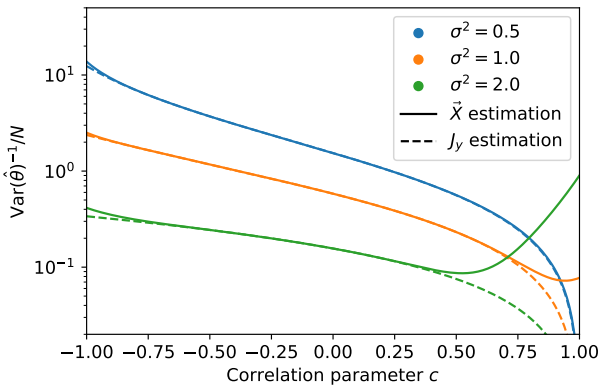

Figure 5: Asymptotic estimator variance calculated using Eq. (71) for the Rouwenhorst process with $M = 3$ phases state space with either J_y (dashed lines) or higher moment $\vec{X}$ (solid lines) measurement. Here we use only $\vec{X} = (J_y, X_{1,2})^T$, as including more observables has negligible effect.

For the discretized Rouwenhorst process above, the argument ceases to hold, and for $c > 0$ we can obtain unintuitive results:

$$\lim_{c\to 1}\lim_{N\to\infty}\frac{\mathcal{F}_Q^{(N)}}{N} \neq 0, \tag{72}$$

whereas for the original Markovian Gaussian process, CS bound (30) tells us, that the first limit should be equal to 0. Moreover, for $c \gg 0$, increasing strength of noise decreases the estimation error, which further questions the accuracy of the approximation. In Fig. 5 we present an example of such behaviour for $M = 3$. We should stress that the discretization method ceases to be a good approximation of a continuously supported process in the strongly correlated regime. Let us note that the order of taking limits in Eq. (72) is important, as any finite N taking $c = 1$ allows for Heisenberg scaling.

References

[1] Vittorio Giovannetti, Seth Lloyd, and Lorenzo Maccone. "Quantum-Enhanced Measurements: Beating the Standard Quantum Limit". Science **306**, 1330–1336 (2004). arXiv:quant-ph/0412078.

[2] Vittorio Giovannetti, Seth Lloyd, and Lorenzo Maccone. "Advances in quantum metrology". Nat. Photonics **5**, 222–229 (2011). arXiv:1102.2318v1.

[3] Rafał Demkowicz-Dobrzański, Marcin Jarzyna, and Jan Kołodyński. "Quantum Limits in Optical Interferometry". In Emil Wolf, editor, Progress in Optics, Volume 60. Pages 345–435. Elsevier, Amsterdam (2015). arXiv:1405.7703.

[4] C. L. Degen, Friedemann Reinhard, and Paola Cappellaro. "Quantum sensing". Rev. Mod. Phys. **89**, 035002 (2017). arXiv:1611.02427.

[5] Luca Pezzè, Augusto Smerzi, Markus K. Oberthaler, Roman Schmied, and Philipp Treutlein. "Quantum metrology with nonclassical states of atomic ensembles". Rev. Mod. Phys. **90**, 035005 (2018). arXiv:1609.01609.

[6] Stefano Pirandola, B Roy Bardhan, Tobias Gehring, Christian Weedbrook, and Seth Lloyd. "Advances in photonic quantum sensing". Nature Photonics **12**, 724–733 (2018). url: https://doi.org/10.1038/s41566-018-0301-6.

[7] Emanuele Polino, Mauro Valeri, Nicolò Spagnolo, and Fabio Sciarrino. "Photonic quantum metrology". AVS Quantum Sci. **2**, 024703 (2020). arXiv:2003.05821.

[8] Jing Liu, Mao Zhang, Hongzhen Chen, Lingna Wang, and Haidong Yuan. "Optimal Scheme for Quantum Metrology". Adv Quantum Tech **5**, 2100080 (2022). arXiv:2111.12279.

[9] Lin Jiao, Wei Wu, Si-Yuan Bai, and Jun-Hong An. "Quantum Metrology in the Noisy Intermediate-Scale Quantum Era". Adv Quantum TechPage 2300218 (2023). arXiv:2307.07701.

[10] Qiushi Liu, Zihao Hu, Haidong Yuan, and Yuxiang Yang. "Fully-Optimized Quantum Metrology: Framework, Tools, and Applications". Adv Quantum TechPage 2400094 (2024). arXiv:2409.07068.

[11] Victor Montenegro, Chiranjib Mukhopadhyay, Rozhin Yousefjani, Saubhik Sarkar, Utkarsh Mishra, Matteo G.A. Paris, and Abolfazl Bayat. "Review: Quantum metrology and sensing with many-body systems". Physics Reports **1134**, 1–62 (2025).

[12] Carlton M. Caves. "Quantum-mechanical noise in an interferometer". Phys. Rev. D **23**, 1693–1708 (1981).

[13] Rafal Demkowicz-Dobrzański, Marcin Jarzyna, and Jan Kołodyński. "Chapter four - quantum limits in optical interferometry". In E. Wolf, editor, Progress in Optics. Volume 60 of Progress in Optics, pages 345–435. Elsevier (2015).

[14] Mankei Tsang, Ranjith Nair, and Xiao-Ming Lu. "Quantum theory of superresolution for two incoherent optical point sources". Phys. Rev. X **6**, 031033 (2016).

[15] Alessandro Candeloro, Cristian Degli Esposti Boschi, and Matteo G. A. Paris. "Quantum probes for universal gravity corrections". Phys. Rev. D **102**, 056012 (2020).

[16] Michael A Taylor and Warwick P Bowen. "Quantum metrology and its application in biology". Physics Reports **615**, 1–59 (2016).

[17] Z. Y. Ou. "Fundamental quantum limit in precision phase measurement". Phys. Rev. A **55**, 2598–2609 (1997).

[18] W. Dür, M. Skotiniotis, F. Fröwis, and B. Kraus. "Improved quantum metrology using quantum error correction". Phys. Rev. Lett. **112**, 080801 (2014).

[19] Sisi Zhou, Mengzhen Zhang, John Preskill, and Liang Jiang. "Achieving the Heisenberg limit in quantum metrology using quantum error correction". Nat. Commun. **9**, 78 (2018). arXiv:1706.02445.

[20] B. M. Escher, Ruynet L. de Matos Filho, and Luiz Davidovich. "General framework for estimating the ultimate precision limit in noisy quantum-enhanced metrology". Nat. Phys. **7**, 406–411 (2011). arXiv:1201.1693.

[21] Rafał Demkowicz-Dobrzański, Jan Kołodyński, and Mădălin Guţă. "The elusive Heisenberg limit in quantum-enhanced metrology". Nat. Commun. **3**, 1063 (2012). arXiv:1201.3940.

[22] Rafał Demkowicz-Dobrzański and Lorenzo Maccone. "Using Entanglement Against Noise in Quantum Metrology". Phys. Rev. Lett. **113**, 250801 (2014). arXiv:1407.2934.

[23] Pavel Sekatski, Michalis Skotiniotis, Jan Kołodyński, and Wolfgang Dür. "Quantum metrology with full and fast quantum control". Quantum **1**, 27 (2017). arXiv:1603.08944.

[24] Rafał Demkowicz-Dobrzański, Jan Czajkowski, and Pavel Sekatski. "Adaptive Quantum Metrology under General Markovian Noise". Phys. Rev. X **7**, 041009 (2017). arXiv:1704.06280.

[25] Sisi Zhou and Liang Jiang. "Asymptotic Theory of Quantum Channel Estimation". PRX Quantum **2**, 010343 (2021). arXiv:2003.10559.

[26] Yuichiro Matsuzaki, Simon C. Benjamin, and Joseph F. Fitzsimons. "Magnetic field sensing beyond the standard quantum limit under the effect of decoherence". Phys. Rev. A **84**, 012103 (2011). arXiv:1101.2561.

[27] Alex W. Chin, Susana F. Huelga, and Martin Bodo Plenio. "Quantum Metrology in Non-Markovian Environments". Phys. Rev. Lett. **109**, 233601 (2012). arXiv:1103.1219.

[28] Katarzyna Macieszczak. "Zeno limit in frequency estimation with non-Markovian environments". Phys. Rev. A **92**, 010102 (2015). arXiv:1403.1333v1.

[29] Andrea Smirne, Jan Kołodyński, Susana F. Huelga, and Rafał Demkowicz-Dobrzański. "Ultimate Precision Limits for Noisy Frequency Estimation". Phys. Rev. Lett. **116**, 120801 (2016). arXiv:1511.02708.

[30] Jan F. Haase, Andrea Smirne, Jan Kołodyński, Rafał Demkowicz-Dobrzański, and Susana F. Huelga. "Fundamental limits to frequency estimation: A comprehensive microscopic perspective". New J. Phys. **20**, 053009 (2018). arXiv:1710.04673.

[31] Piotr Szańkowski, M Trippenbach, and J. Chwedeńczuk. "Parameter estimation in memory-assisted noisy quantum interferometry". Phys. Rev. A **90**, 063619 (2014).

[32] A. Smirne, A. Lemmer, M. B. Plenio, and S. F. Huelga. "Improving the precision of frequency estimation via long-time coherences". Quantum Sci. Technol. **4**, 025004 (2019). arXiv:1808.03664.

[33] Dario Tamascelli, Claudia Benedetti, Heinz-Peter Breuer, and Matteo G. A. Paris. "Quantum probing beyond pure dephasing". New J. Phys. **22**, 083027 (2020). arXiv:2003.04014.

[34] Anian Altherr and Yuxiang Yang. "Quantum Metrology for Non-Markovian Processes". Phys. Rev. Lett. **127**, 060501 (2021). arXiv:2103.02619.

[35] Xiaodong Yang, Xinyue Long, Ran Liu, Kai Tang, Yue Zhai, Xinfang Nie, Tao Xin, Jun Li, and Dawei Lu. "Control-enhanced non-Markovian quantum metrology". Commun. Phys. **7**, 282 (2024).

[36] Jan Jeske, Jared H. Cole, and Susana F. Huelga. "Quantum metrology subject to spatially correlated Markovian noise: Restoring the Heisenberg limit". New J. Phys. **16**, 073039 (2014).

[37] David Layden and Paola Cappellaro. "Spatial noise filtering through error correction for quantum sensing". Npj Quantum Inf. **4**, 30 (2018).

[38] Jan Czajkowski, Krzysztof Pawłowski, and Rafał Demkowicz-Dobrzański. "Many-body effects in quantum metrology". New J. Phys. **21**, 053031 (2019).

[39] David Layden, Sisi Zhou, Paola Cappellaro, and Liang Jiang. "Ancilla-Free Quantum Error Correction Codes for Quantum Metrology". Phys. Rev. Lett. **122**, 040502 (2019). arXiv:1811.01450.

[40] David Layden, Mo Chen, and Paola Cappellaro. "Efficient Quantum Error Correction of Dephasing Induced by a Common Fluctuator". Phys. Rev. Lett. **124**, 020504 (2020). arXiv:1903.01046.

[41] Guim Planella, Marina F. B. Cenni, Antonio Acín, and Mohammad Mehboudi. "Bath-Induced Correlations Enhance Thermometry Precision at Low Temperatures". Phys. Rev. Lett. **128**, 040502 (2022).

[42] Félix Beaudoin, Leigh M. Norris, and Lorenza Viola. "Ramsey interferometry in correlated quantum noise environments". Phys. Rev. A **98**, 020102 (2018).

[43] Francisco Riberi, Leigh M. Norris, Félix Beaudoin, and Lorenza Viola. "Frequency es-

timation under non-Markovian spatially correlated quantum noise: Restoring superclassical precision scaling". New J. Phys. **24**, 103011 (2022). arXiv:2204.10798.

[44] Akio Fujiwara and Hiroshi Imai. "A fibre bundle over manifolds of quantum channels and its application to quantum statistics". J. Phys. A **41**, 255304 (2008).

[45] Jan Kołodyński and Rafał Demkowicz-Dobrzański. "Efficient tools for quantum metrology with uncorrelated noise". New J. Phys. **15**, 073043 (2013). arXiv:1303.7271.

[46] Sisi Zhou and Liang Jiang. "Optimal approximate quantum error correction for quantum metrology". Phys. Rev. Res. **2**, 013235 (2020). arXiv:1910.08472.

[47] Stanisław Kurdziałek, Wojciech Górecki, Francesco Albarelli, and Rafał Demkowicz-Dobrzański. "Using adaptiveness and causal superpositions against noise in quantum metrology". Phys. Rev. Lett. **131**, 090801 (2023).

[48] Yuxiang Yang. "Memory Effects in Quantum Metrology". Phys. Rev. Lett. **123**, 110501 (2019). arXiv:1904.07267.

[49] Qiushi Liu, Zihao Hu, Haidong Yuan, and Yuxiang Yang. "Optimal Strategies of Quantum Metrology with a Strict Hierarchy". Phys. Rev. Lett. **130**, 070803 (2023). arXiv:2203.09758.

[50] Qiushi Liu and Yuxiang Yang. "Efficient tensor networks for control-enhanced quantum metrology". Quantum **8**, 1571 (2024). arXiv:2403.09519.

[51] Stanislaw Kurdzialek, Piotr Dulian, Joanna Majsak, Sagnik Chakraborty, and Rafal Demkowicz-Dobrzanski. "Quantum metrology using quantum combs and tensor network formalism". New Journal of Physics (2025).

[52] Stanisław Kurdziałek, Francesco Albarelli, and Rafał Demkowicz-Dobrzański. "Universal bounds for quantum metrology in the presence of correlated noise". Phys. Rev. Lett. **135**, 130801 (2025).

[53] Arpan Das and Rafał Demkowicz-Dobrzański. "Quantum metrology in presence of correlated noise via markovian embedding" (2025). arXiv:2509.19685.

[54] S. F. Huelga, C. Macchiavello, T. Pellizzari, A. K. Ekert, M. B. Plenio, and J. I. Cirac. "Improvement of frequency standards with quantum entanglement". Phys. Rev. Lett. **79**, 3865–3868 (1997).

[55] Duger Ulam-Orgikh and Masahiro Kitagawa. "Spin squeezing and decoherence limit in ramsey spectroscopy". Phys. Rev. A **64**, 052106 (2001).

[56] Leonard S. Ornstein and George E. Uhlenbeck. "On the theory of the brownian motion". Physical Review **36**, 823–841 (1930).

[57] John K. Stockton, J. M. Geremia, Andrew C. Doherty, and Hideo Mabuchi. "Robust quantum parameter estimation: Coherent magnetometry with feedback". Phys. Rev. A **69**, 032109 (2004).

[58] Vivi Petersen and Klaus Mølmer. "Estimation of fluctuating magnetic fields by an atomic magnetometer". Phys. Rev. A **74**, 043802 (2006).

[59] Júlia Amorós-Binefa and Jan Kołodyński. "Noisy atomic magnetometry in real time". New Journal of Physics **23**, 123030 (2021).

[60] Julia Amoros-Binefa, Morgan W. Mitchell, and Jan Kolodynski. "Tracking time-varying signals with quantum-enhanced atomic magnetometers" (2025). arXiv:2503.14793.

[61] Robert Stelzer. "Carma processes driven by non-gaussian noise" (2011). arXiv:1201.0155.

[62] Danijel Grahovac and Magdalena Mikić. "Superpositions of carma processes" (2026). arXiv:2601.15796.

[63] Giulio Chiribella, Giacomo Mauro D'Ariano, and Paolo Perinotti. "Theoretical framework for quantum networks". Phys. Rev. A **80**, 022339 (2009).

[64] Carl W. Helstrom. "Quantum detection and estimation theory". Academic Press. New York (1976).

[65] Samuel L. Braunstein and Carlton M. Caves. "Statistical distance and the geometry of quantum states". Phys. Rev. Lett. **72**, 3439–3443 (1994).

[66] Krzysztof Chabuda, Jacek Dziarmaga, Tobias J. Osborne, and Rafał Demkowicz-Dobrzański. "Tensor-network approach for

quantum metrology in many-body quantum systems". Nat. Commun. **11**, 250 (2020). arXiv:1906.02761.

[67] Masahiro Kitagawa and Masahito Ueda. "Squeezed spin states". Phys. Rev. A **47**, 5138–5143 (1993).

[68] Jian Ma, Xiaoguang Wang, C.P. Sun, and Franco Nori. "Quantum spin squeezing". Physics Reports **509**, 89–165 (2011).

[69] Arkadiusz Kobus and Rafał Demkowicz-Dobrzański. "Asymptotically optimal joint phase and dephasing strength estimation using spin-squeezed states" (2025). arXiv:2507.22997.

[70] Keiji Matsumoto. "On metric of quantum channel spaces" (2010). arXiv:1006.0300.

[71] Marco Radaelli, Gabriel T Landi, Kavan Modi, and Felix C Binder. "Fisher information of correlated stochastic processes". New Journal of Physics **25**, 053037 (2023).

[72] Katarzyna Macieszczak. "Upper bounds on the quantum fisher information in the presence of general dephasing" (2014). arXiv:1403.0955.

[73] Giulio Chiribella, Giacomo M. D'Ariano, and Paolo Perinotti. "Memory Effects in Quantum Channel Discrimination". Phys. Rev. Lett. **101**, 180501 (2008).

[74] Karen A. Kopecky and Richard M.H. Suen. "Finite state markov-chain approximations to highly persistent processes". Review of Economic Dynamics **13**, 701–714 (2010).

[75] Piotr Dulian, Stanisław Kurdziałek, and Rafał Demkowicz-Dobrzański. "Qmetro++". https://github.com/pdulian/qmetro (2025).

[76] https://github.com/Arkadiusz-Kobus/Optimal-phase-estimation-in-the-presence-of-correlated-dephasing.

[77] B. Porat and B. Friedlander. "Computation of the exact information matrix of gaussian time series with stationary random components". IEEE Transactions on Acoustics, Speech, and Signal Processing **34**, 118–130 (1986).

[78] J.M. Bogoya, A. Böttcher, S.M. Grudsky, and E.A. Maximenko. "Eigenvectors of hermitian toeplitz matrices with smooth simple-loop symbols". Linear Algebra and its Applications **493**, 606–637 (2016).

[79] Leon Isserlis. "On a formula for the product-moment coefficient of any order of a normal frequency distribution in any number of variables". Biometrika **12**, 134–139 (1918).

[80] Jack Sherman and Winifred J. Morrison. "Adjustment of an inverse matrix corresponding to a change in one element of a given matrix". The Annals of Mathematical Statistics **21**, 124–127 (1950). url: http://www.jstor.org/stable/2236561.